JOURNAL OF APPLIED ELECTROCHEMISTRY 19 (1989) 434–442

Electrochemically initiated (co)polymerization of acrylamide and acrylonitrile on a steel cathode – electrochemical and impedance study

T. GRCHEV, M. CVETKOVSKA

'Cyril and Methodius' University, Faculty of Technology and Metallurgy, 9100 Skopje, Yugoslavia

Received 10 October 1987; revised 23 July 1988

Investigations were carried out into the processes of electrochemically initiated (co)polymerization (EIP) of acrylamide (AA) and/or acrylonitrile (AN) from acidic aqueous solutions on a steel cathode. The aim was to obtain (co)polymer films with given electroinsulating and corrosion protection properties. The kinetics of (co)polymer film formation were investigated using various electrochemical methods (constant current and constant potential electrolysis, cyclic voltammetry, double-layer capacity measurements) and ellipsometry. The electrical properties of the films formed were studied (*ex situ*) by measuring their impedance (Z) and phase angle (θ) as a function of frequency. It was shown that equivalent circuit (EC), proposed for covered metal surfaces in solutions, can be satisfactorily applied. The values of the EC elements obtained by curve fitting to experimental results show the influence of the thermal treatments and/or moisture concentration on the impedance characteristics of polymer films. The mechanism of (co)polymer film formation as well as the electrical and corrosion protection properties are discussed with regard to the experimental parameters and some characteristics of the films obtained.

1. Introduction

The processes of electrochemically initiated polymerization (EIP) of acrylamide (AA) and acrylonitrile (AN) on metal surface have been extensively studied in the last 10 years [1–8]. It was found that two different mechanisms (direct and indirect) exist for the initiation of the polymerization at the metal surface. The first assumes a metal ion–monomer complex formation in the solution (e.g. $ZnOH^+$–AA) and its reduction at the cathode with formation of radicals [1–3]. The other mechanism [6–8] suggests monomer radical formation via adsorbed H atoms (e.g. $H–M^\cdot$) which initiates polymerization.

In this work, an attempt is made to follow the kinetics of (co)polymer film formation on a metal surface, and to obtain some additional information about the mechanism of the processes and the electrical properties of the films. Processes of EIP of AA and copolymerization of AA and AN from acidic aqueous solutions on a steel cathode were studied using classical electrochemical methods, impedance measurements and ellipsometry.

2. Experimental details

EIP of AA was carried out in the presence of N, N'-methylenbisacrylamide (MBAA) and $ZnCl_2$ as well as copolymerization of AA and AN in sulphuric acid solutions on a steel cathode. A classical, three-compartment electrochemical cell was used which was thermostated at 30° C. Solutions were prepared from reagent grade chemicals (Merck) with p.a. purity and redistilled water. Acrylamide was twice recrystallized from benzene (84–85° C); acrylonitrile was redistilled at 86° C after removal of the inhibitor, and $ZnCl_2$ and H_2SO_4 were used without any additional purification.

The working electrode was a steel cylinder (AISI 316), placed in a Teflon holder with exposed flat area of $2\,cm^2$ ($d = 16\,mm$). Saturated calomel and Hg/Hg_2SO_4 reference electrodes and a Pt foil (ca $24\,cm^2$) as auxiliary electrode, were used. All potentials in this paper are referred to the saturated calomel electrode (SCE). The steel electrode was mechanically polished with silicon papers and, for ellipsometric measurements only, it was repolished with Al_2O_3 suspension down to $1\,\mu m$.

An Electrochemistry System (PAR 170) and a Tacussel Integrator (IG-6) were used for all electrochemical measurements and a Hewlett Packard impedance meter (Model 4800 A) was used for *ex situ* measurements on the polymer films. A Rudolph Research ellipsometer (43603-200) with an optical cell was used for ellipsometric measurements. Double-layer capacity measurements were carried out using the method proposed by Schultze *et al.* [9].

3. Results and discussion

3.1. *System: AA-$ZnCl_2$*

EIP of AA in the presence of $ZnCl_2$ on a steel cathode is a well-known process [1–4]. It was shown that the mechanism of AA polymerization is free radical [3].

0021-891X/89 $03.00 + .12

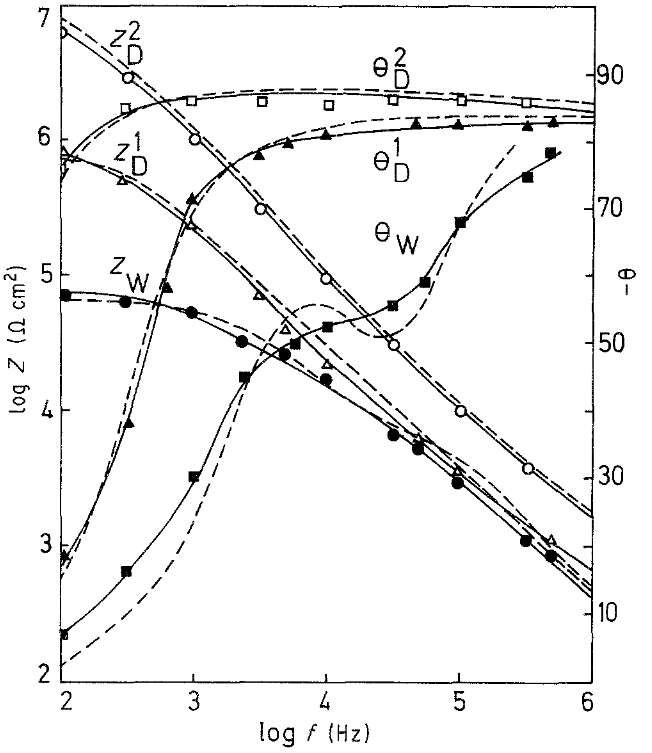

Fig. 1. Bode plots for PAA films (20 μm thick) on steel surfaces obtained in *ex situ* conditions; (——) experimental and (- - -) theoretical curves for wet (w), semi-dry (D1) and dry (D2) polymer films (see Table 1).

The obtained polyacrylamide (PAA) film is in a gel form. After a short treatment in acetone and drying at room temperature it transforms into a homogeneous, white, water-soluble one with thickness of 5–50 μm. The films in a hydrogel form have a limited application; prevention of coagulation of blood in steel tanks, imobilization of enzymes in bioreactors, facilitation of transport of fluids through tubes, etc. Thus, it is of interest to obtain a water-insoluble film directly without any additional chemical and/or thermal treatment, and to find suitable methods to follow the film formation process as well as to determine the impedance characteristics of the film formed. In this paper some of our experimental results are presented for EIP of AA in the presence of $ZnCl_2$ and MBAA, in order to obtain cross-linked films.

The films were obtained from solutions containing 4 M AA, 0.15 M $ZnCl_2$ and 0.1 M MBAA, pH 4.6–4.8, at 30° C with a constant current electrolysis, $j = 5\,\mathrm{mA\,cm^{-2}}$, on a steel cathode for 10–60 s. The thicknesses of these films, determined by gravimetry (PAA density 1.23), range from 10 to 50 μm.

Ex situ measurements over a wide frequency range determined the impedance characteristics of the polymer films obtained. Some of the experimentally obtained results, presented in Fig. 1 show that the impedance characteristics of PAA films are mainly determined by the presence of water in the polymer film and/or at the metal–polymer interface, and depends strongly on the drying procedure. Similar Bode plots have been obtained in the impedance studies of covered metal surfaces with polymer films in corrosive aqueous media as a function of a treatment time [13, 16]. The penetration of water molecules and/or ions into pores or defect sites of the film drastically changes the impedance and phase angle also. The resistance of the film decreases and its capacity increases as a result of increases in the dielectric constant of the 'wet' polymer film and/or through the influence of a double-layer capacity in the pores. For such a case an equivalent circuit (EC) has been proposed which explains the experimental results satisfactorily [12–16]. In our case a very similar EC can be applied (Fig. 2). The component, $R_{\rm pf}$, resistance of the intact polymer film was added in this case

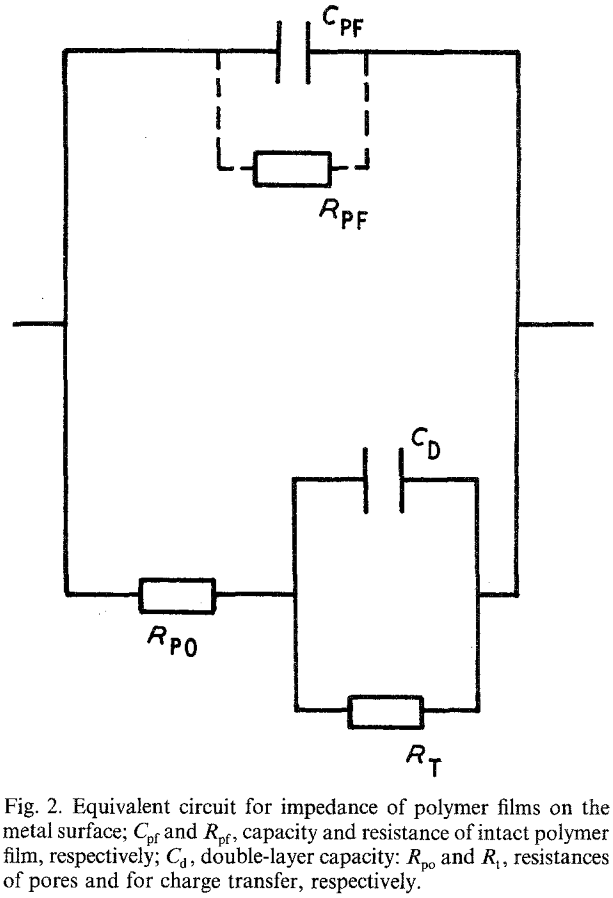

Fig. 2. Equivalent circuit for impedance of polymer films on the metal surface; $C_{\rm pf}$ and $R_{\rm pf}$, capacity and resistance of intact polymer film, respectively; $C_{\rm d}$, double-layer capacity: $R_{\rm po}$ and $R_{\rm t}$, resistances of pores and for charge transfer, respectively.

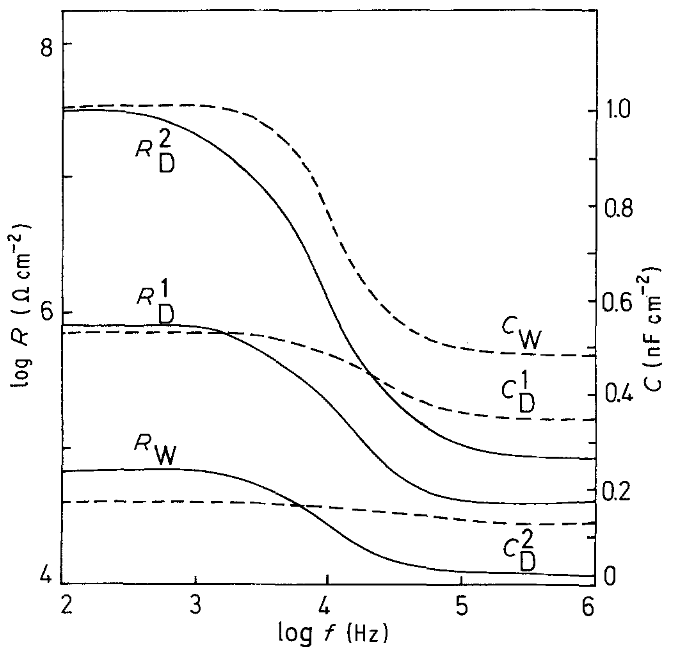

Fig. 3. R–C components of the PAA films as obtained for theoretical curves presented in Fig. 1 and Table 1.

but, as will be shown, its influence is small and appears at high frequencies.

Figure 1 shows a fitting procedure of the experimentally obtained results, using the proposed EC (Fig. 2). Good agreement between experiment and model was found for 'semi-dry' and dry PAA films and it was satisfactory for a 'wet' PAA film (Fig. 1). In the case of a wet PAA film, the existence of two RC time constants is more pronounced on the theoretical curves. The values of the EC components for theoretical curves for best fitting with the experimental data are presented in Table 1. It can be concluded that the values of the double-layer capacity, C_d, decrease in order: $C^{w\text{-}d} > C_d^{D1} > C_d^{D2}$, which is reasonable. In the case of a wet PAA film the contribution of capacity on the metal–moisture interface is dominant and decreases with drying. On the other hand, the resistance of pores, R_{po}, increases in the order: $R_{po}^{w} < R_{po}^{D1} < R_{po}^{D2}$ which depends on the moisture concentration and number (and/or size) of pores in the polymer film.

A considerable difference between R_{po}^{D1} and R_{po}^{D2} shows that, even after 24 h drying at room temperature, the polymer film contains some moisture which can be eliminated at elevated temperatures. The values of R_t double layer resistance for charge transfer, also shown an acceptable behaviour.

The influence of various drying treatments of the PAA films can be also seen from Fig. 3. The log R(and/or C)–log f curves for a theoretical model, Table 1, show an S-shaped behaviour indicating the influence of two parallel RC circuits or two RC time constants. Capacities strongly depend on the moisture concentration in the polymer films which can also be seen from the estimated values of dielectric constants: $D_w = 22$, $D_{D1} = 12$ and $D_{D2} = 3.85$ (for the lower frequency range, Fig. 3). These values seem to be reasonable, compared with some literature data [16] and taking into account the strong influence of moisture. The dielectric constant of a dry polymer film (D2) is mainly determined by C_{pf} and thus the C_d–R_{po} circuit, Fig. 2, has a negligible influence. So, the impedance behaviour of a dry polymer film (D2) can be satisfactorily fitted with a simple parallel circuit ($R_{pf} = 3.5 \times 10^7\,\Omega\,\text{cm}^2$ and $C_{pf} = 0.17\,\text{nF}\,\text{cm}^{-2}$).

The value of the $\text{d}(Z)/\text{d}\log f$ slope, very close to -1 for a dry polymer film (D2) (Fig. 1), also indicates a parallel RC circuit. Wet and semi-dry polymer films (w and D1) have $\text{d}(Z)/\text{d}\log f$ slopes from -0.75 to -0.80 indicating the influence of moisture, and perhaps, a small influence of a Warburg impedance.

From Nyquist plots (Figs. 4 and 5) it can also be concluded that in the case of a wet PAA film (w) the influence of a second parallel EC (R_t–C_d) cannot be

Table 1. Values of the EC components for best fitting with experiment

No. of sample	*PAA film*	C_{pf} (*nF cm*$^{-2}$)	C_d (*nF cm*$^{-2}$)	R_{pf} (*k*Ω *cm*^{2})	R_{po} (*k*Ω *cm*^{2})	R_t (*k*Ω *cm*^{2})
1	20 μm; wet (w)	0.30	1.00	350	12	70
2	20 μm; dry (D1)	0.35	0.20	10^4	40	800
3	20 μm; dry (D2)	0.13	0.04	2.5×10^5	150	3.5×10^4
4	50 μm; dry (D1)	0.08	0.06	10^5	120	2000

w: PAA film in a gel form after a treatment in acetone for 30 s is dried at room temperature for 2 h.
D1: Same as w but dried at room temperature for 24 h.
D2: same as w but dried at 455° C for 6 h.

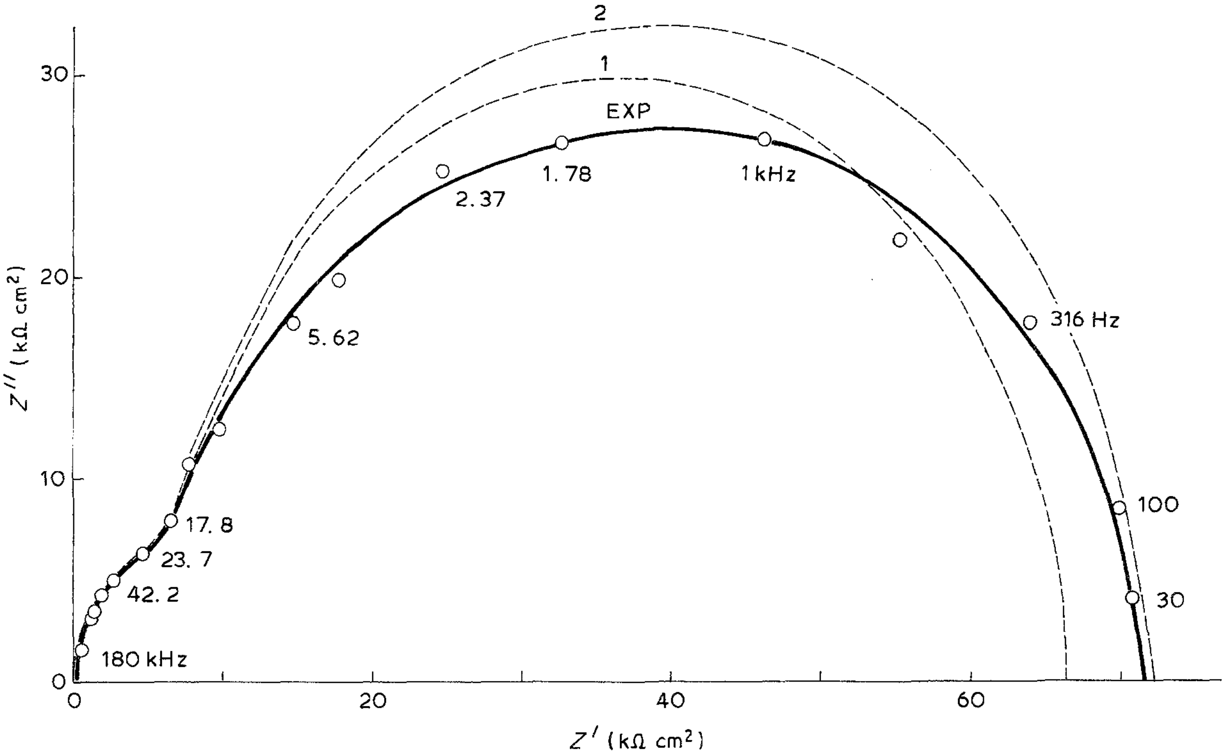

Fig. 4. Nyquist plots for a wet PAA film; (——) experimentally obtained and (- - -) for an EC (Fig. 2); curve (1): C_{pf} = 0.30 and C_d = 1.0 nF cm^{-2}, R_{pf} = 350, R_{po} = 12 and R_t = 70 kΩ cm²; curve (2): without R_{pf} in the EC and R_t = 60 kΩ cm².

neglected and for a semi-dry film (D1) this influence strongly decreases. A fairly good agreement between the theoretical model and experimental results can be seen from these figures. In the case of a wet PAA film (Fig. 4) the RC time constants have values: $\tau_m = R_tC_d = 7 \times 10^{-5}$ s and $\tau_{pf} = R_{pf}C_{pf} = 3.8 \times 10^{-6}$ s. According to theoretical considerations [14] the τ_m/τ_{pf} and R_t/R_{pf} ratios have limiting values for a quantitative resolution of the two (Z'-Z'') semi-circles. In the case of a semi-dry film (D1) the second condition

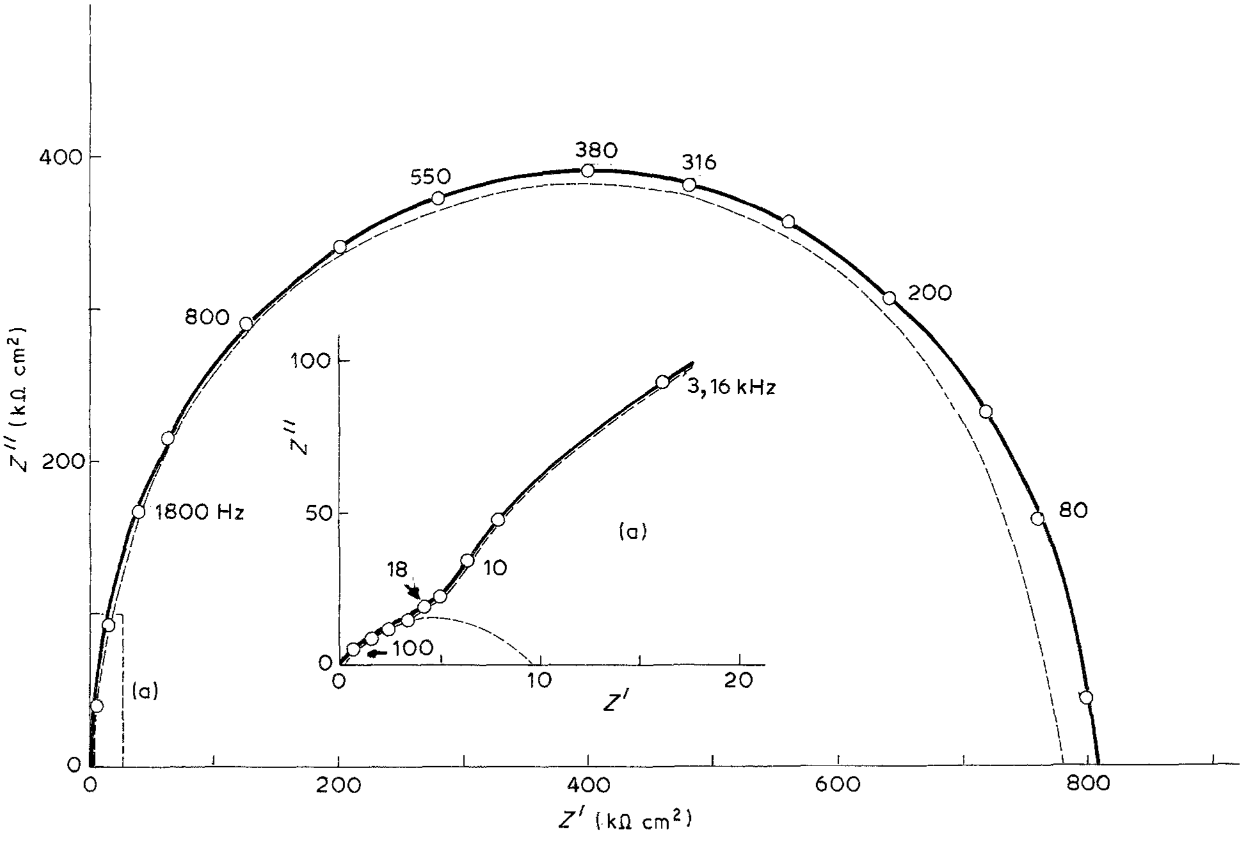

Fig. 5. Nyquist plots for a semi-dry PAA film (D1). Theoretical curve (- - -) is obtained for C_{cf} = 0.35 and c_d = 0.20 nF cm^{-2}, R_{pf} = 10 MΩ cm², R_{po} = 40 and R_t = 800 kΩ cm².

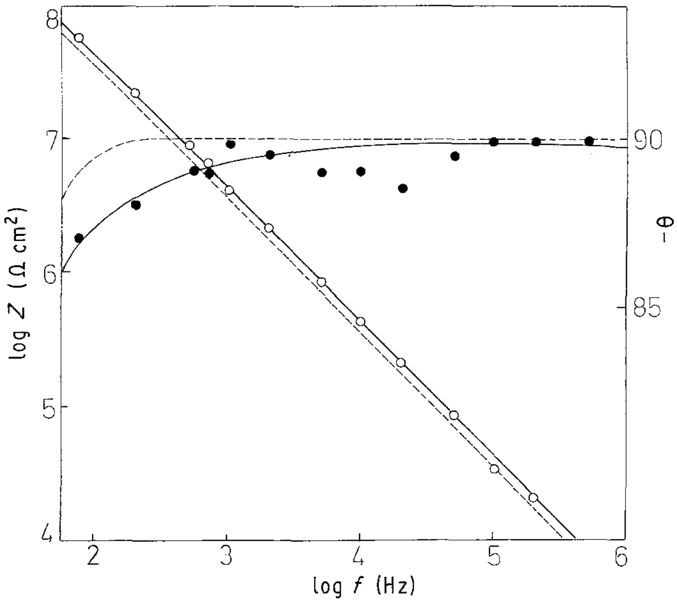

Fig. 6. Bode plots for polyethylene foil (40 μm thick). Theoretical curves are obtained for a simple parallel EC: $C_{pf} = 45\,pF\,cm^{-2}$ and $R_{pf} = 5 \times 10^9\,\Omega cm^2$.

($R_t/R_{p0} \leqslant 5$) is not fulfilled and the resolution is rendered more difficult. A fairly good agreement between theoretical and experimental (Z'–Z'') maximum frequencies, in both cases, can be used as an additional argument for a correct fitting ($f^1_{max} = 1/2\pi R_t C_d$ and $f^2_{max} = 1/2\pi R_{po} C_{pf}$).

The impedance characteristics of an polyethylene foil (40 μm thick) are shown in Fig. 6. In this case the influence of moisture in the film can be neglected. As can be seen from this figure a linear log Z–log f plot with a slope of -1 and phase angle values between $-87°$ and $-90°$ is obtained. A simple parallel EC with $R_{pf} = 5 \times 10^9\,\Omega cm^2$ and $C_{pf} = 45\,pF\,cm^{-2}$ shows good agreement with experiment (Fig. 6). Thus, the estimated value of polyethylene dielectric constant ($D_{pe} = 2.04$) and its volume-specific resistance ($1.25 \times 10^{12}\,\Omega cm$) show very good agreement with literature data.

3.2. *System: AA–AN–H_2SO_4*

The process of EIP of AA and AN on a metal surface from acidic aqueous solution of H_2SO_4 (0.025 M) has been investigated over a long period [6–8]. It was assumed that the initiation of (co)polymerization takes place via adsorbed H atoms (radicals) according to the reactions:

$$H^+ + e = H_{ads} \tag{1}$$

$$H_{ads} + M = H\text{–}M^{\cdot} \quad (M, \text{monomer}) \tag{2}$$

The aim of our further study was to obtain some additional information and/or proof for the proposed mechanism of initiation of the copolymerization on the electrode surface. This was to assist us in determining the kinetics of film formation and electrical and corrosion protection properties of the films formed. Electrochemical experiments (constant potential and constant current electrolysis) combined with ellipsometry have shown that a copolymer film on the steel cathode is formed over a wide potential range (from -0.7 to -2.2 V/SCE) and/or at constant currents from -5 to $-30\,mA\,cm^{-2}$. Evidently, under these electrochemical conditions, only a hydrogen evolution reaction takes place. In the presence of monomers (AA and AN, 1.5 M each) the rate of this reaction ($2H^+ + 2e = H_2$) is lower due to the increased solution viscosity and copolymer film formation on the metal surface. Taking into account that PAA–PAN films are formed even at -0.7 V (reduction potentials of these monomers are > -1.9 V) we may suppose that some of the electrochemically generated species, such as H_{ads}, can take part in the initiation of the polymerization at the metal surface.

The kinetics of the copolymer film formation on a steel cathode was followed using several electrochemical methods and ellipsometry. Voltammograms for the hydrogen evolution reaction on a metal and/or metal–polymer surfaces can be used as an indication of the kinetics of copolymer film formation (Fig. 7). The copolymer (PAA–PAN) film was formed at -1.2 V (for 15–120 min) and subsequently cathodic voltammograms were recorded. As can be seen from this figure hydrogen current peaks strongly depend upon the time of film formation. In this case the hydrogen evolution reaction takes place, mainly at the uncovered metal surface and/or in the film pores. Taking into account the thickness of the copolymer film formed for 120 min (ca 7 μm), and the assumption of a pore-free film, a limiting hydrogen current of 0.1–0.5 $\mu A\,cm^{-2}$ ($D_{H^+} \geqslant 10^{-10}\,cm^2\,s^{-1}$, through the film) can be expected. Evidently the hydrogen current, even after 120 min of film formation, is several hundreds of μA, thus indicating the presence of pores. The value of metal surface coverage with polymer film can be roughly determined using the equation:

$$\theta = (j^p_o - j_t)/j^p_o \tag{3}$$

where j^p_o is a value of a hydrogen peak current on a bare metal surface ($t = 0$) and j_t is a corresponding

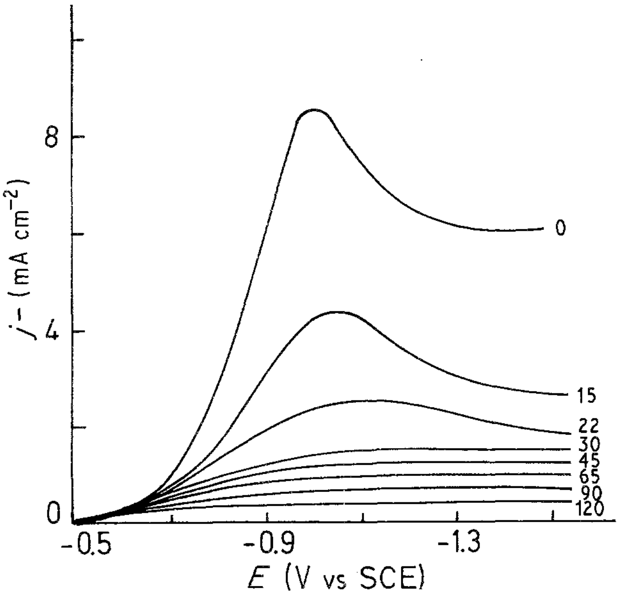

Fig. 7. Voltammograms for hydrogen evolution reaction on a steel electrode (dE/dt = 10 mV s^{-1}) from aqueous solution of 0.025 M H_2SO_4 containing 1.5 M AA and AN (each) as a function of time of copolymer film formation at −1.2 V.

current after a copolymer film formation over a time t. Thus, for a 15 min film formation at −1.2 V, $\theta = 0.5$ and for 120 min $\theta = 0.96$.

It may be noticed that for a period between 1 and ca 10 min of film formation at −1.2 V, almost no differences on the hydrogen voltammograms were observed.

The kinetics of (co)polymer film formation on a steel cathode was also followed by double-layer capacity measurements (at 1 kHz and 2 mV signal) as a function of potential. As can be seen from Fig. 8, the initial value of capacity of steel in 0.025 M H_2SO_4 and 1.5 M AA and AN (each) is low due to the monomer adsorption at the metal–solution interface. In the absence of monomers the capacity of steel in 0.025 M H_2SO_4 is 15–20 μF cm^{-2}. Thus, the initial small increases of the capacity, in the first 10 min, can be explained by metal oxide reduction and/or a small desorption of monomers. A further sharp decrease of capacity, especially at more cathodic potentials, is a result of a copolymer film formation. In this case metal–solution (in the pores), metal–polymer and polymer–solution interfaces exist. Evidently, only the capacities of the metal–polymer (C_{pf}) and metal–solution (C_d) interfaces give a contribution to the measured value. The capacity of the polymer film depends on the film thickness and its dielectric constant. A relatively high capacity value, 0.1–0.25 μF cm^{-2} (Fig. 8), even after 40 min (film thickness ca 2 μm) can be explained by the formation of a porous film. In that case the capacity value can be expressed by the following equation:

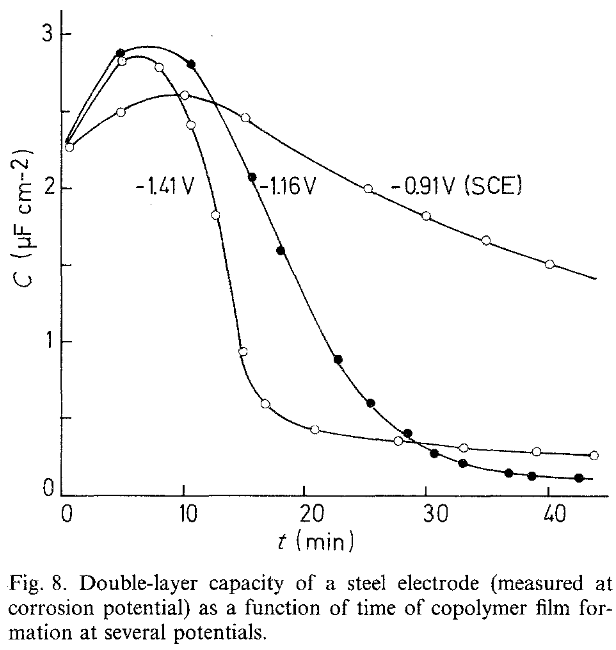

Fig. 8. Double-layer capacity of a steel electrode (measured at corrosion potential) as a function of time of copolymer film formation at several potentials.

$$C = C_d + C_{pf} = (1 - \theta)C_d + \theta D_{pf}/L_{pf} \quad (4)$$

where D_{pf} is the dielectric constant of the copolymer film and θ is the degree of surface coverage with copolymer film.

Using a porous film model, voltammogram for the hydrogen evolution reaction (Fig. 7) and the capacity–time curves (Fig. 8) can be explained. Taking into account the value of a wet copolymer film dielectric constant of about 25 and a thickness between 0.1 and 2 μm the second term in Equation 4 can be neglected ($0.02 < \theta < 1$; $(1 - \theta)C_d \gg \theta D_{pf}/L_{pf}$) and the following equation can be derived

$$\theta = 1 - (C/C_d) \quad (5)$$

where C is the capacity of the film-covered electrode or experimentally measured capacity at time t and C_d is the double-layer capacity of the metal–solution interface (for $\theta = 0$ and/or $t = 0$). This equation is in very good agreement with a Frumkin model of parallel condensers for the adsorption of organic molecules:

$$\theta = (C_{\theta=0} - C)/(C_{\theta=0} - C_{\theta=1}) \quad (6)$$

taking into account that in our case $C_{\theta=1} \ll C_{\theta=0}$ (where $C_{\theta=1}$ is ca 0.15 and $C_{\theta=0}$ is ca 2.8 μF cm^{-2}).

On the basis of the experimentally obtained results (Fig. 8 and Equation 5), it is possible to calculate the coverage–time dependencies (Fig. 9). As can be seen from this figure, the limiting value of a metal surface coverage with polymer film is high (0.9–0.96) and an induction period of about 10 min exists. The kinetics of the surface coverage with a copolymer film depends on the electrode potential (Fig. 9); the limiting value of surface coverage, however, is somewhat higher at the lower potential. In this case we have to conclude that at the higher rates of metal surface covering with a polymer film (more cathodic potentials) the possibility of pore formation is higher.

For the initial periods of film formation linear C–t and/or θ–t plots are obtained (Figs 8 and 9), which strongly depend on the potential of film formation. It can be assumed that in this period a two-dimensional film growth takes place. The film thickness during this period is mainly dependent on the polymer molecular weight. After this period a growth of the previously

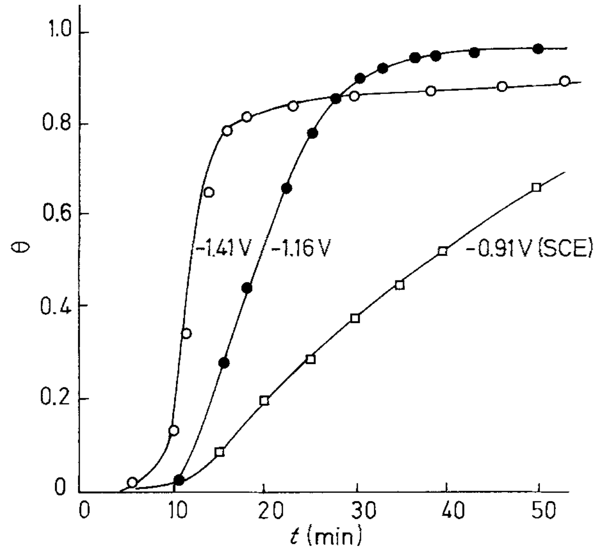

Fig. 9. Coverage–time dependences for a copolymer film formation on a steel cathode (using Equation 5 and Fig. 8).

formed polymer patches occurs in the region of the slightly decreasing capacity.

The kinetics of copolymer film formation on a steel cathode, followed by ellipsometry (Fig. 10), show a significant difference in the rates of PAA, PAN and PAA–PAN film formation. On the other hand, the rate of PAA film formation in the presence of $ZnCl_2$ (followed by a weight method), is about 10^3 times higher. The reason for such a behaviour is a substantial difference in the initiation mechanism of the polymerization processes.

The ellipsometrically determined complex index of refraction ($\hat{n} = n - jk$) of these copolymer films is:

$$\hat{n} = (1.37 - 1.42) - j(0.01 - 0.015) \qquad (7)$$

which indicates ($k = 0.01 - 0.015$) a very low electronic conductivity of the copolymer film. In this case (Fig. 10), the previously observed induction period of about 10 min was confirmed.

Ex situ impedance measurements of the copolymer films obtained at -1.2 and -1.4 V (for 180 min) (Fig. 11), indicate that the film formed at a higher potential has slightly higher values of impedances in all the frequency ranges studied and has somewhat more pronounced differences on the θ–log f plots.

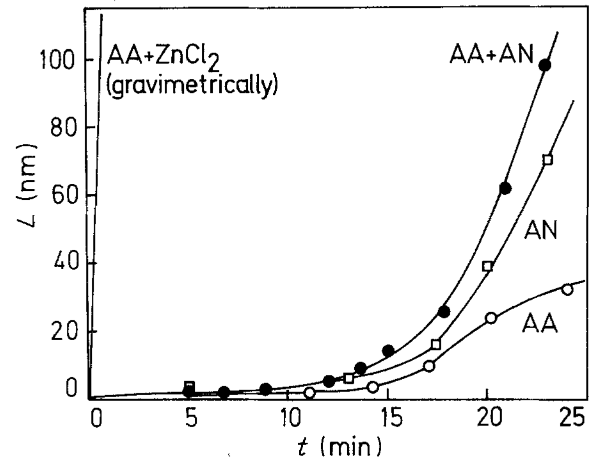

Fig. 10. Kinetics of (co)polymer film formation on a steel cathode at -1.2 V, followed by ellipsometry.

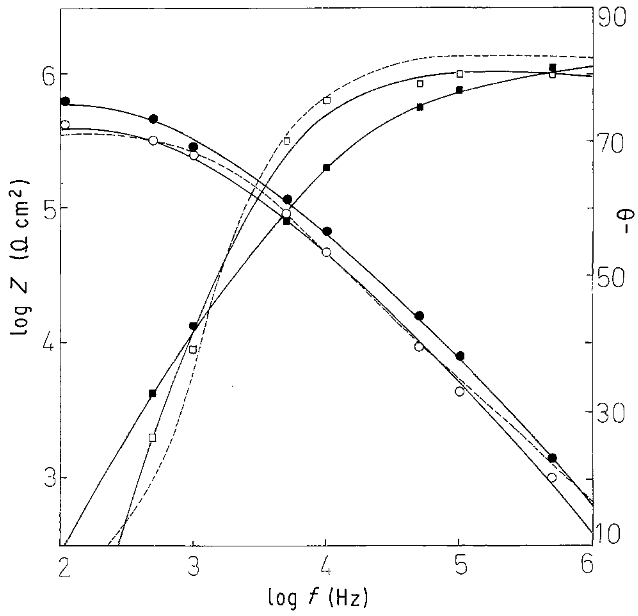

Fig. 11. Bode plots for copolymer films (PAA–PAN) obtained at -1.2 V (—○—) and -1.4 V (—●—) for 3 h; film thickness 10 μm. Theoretical curves (- - -) are obtained for: $C_{pf} = 0.22$ and $C_d = 0.12\,\text{nF cm}^{-2}$, $R_{pf} = 2\,\text{M}\Omega\,\text{cm}^2$, $R_{po} = 12$ and $R_t = 400\,\text{K}\Omega\,\text{cm}^2$.

On the other hand, fairly good linear log Z–log f plots are obtained for $f > 1$ kHz with a slope very close to -1. A theoretical curve was obtained using a previously described EC (Fig. 2) for the following values of the circuit elements: $C_{pf} = 0.22$ and $C_d = 0.12\,\text{nF cm}^{-2}$, $R_{pf} = 2\,\text{M}\Omega\,\text{cm}^2$, $R_{po} = 12\,\text{k}\Omega\,\text{cm}^2$ and $R_t = 400\,\text{k}\Omega\,\text{cm}^2$. A better agreement was found for the copolymer film formed at -1.2 V.

A fairly good agreement, which can be expected from the slope values, was also obtained for a simple parallel circuit: $C_{pf} = 0.33\,\text{nF cm}^{-2}$ and $R_{pf} = 350\,\text{k}\Omega\,\text{cm}^2$. Thus, it can be concluded that copolymer films contain a very low concentration of moisture (low hygroscopy) without any additional thermal treatment. As can be seen from Fig. 12 the above mentioned considerations were confirmed. A well-defined semi-circle without considerable deviations at higher frequencies was experimentally obtained and a reasonable matching of the shape of the curves as well as values of Z' and Z'' at specific frequencies is achieved.

The corrosion protection properties of copolymer films, obtained at various constant potentials and durations of the film formation process, were determined in aerated 3% NaCl solution for a 24 h treatment. The rate of corrosion was determined using a standard phenantroline–spectrophotometric method for determination of Fe^{2+} concentration in the solution. The corrosion protection efficiency of the copolymer films (η_p) is defined as:

$$\eta_p = [m^{o}_{Fe} - m^{pf}_{Fe})/m^{o}_{Fe}]\ 100\% \qquad (8)$$

where m^{o}_{Fe} and m^{pf}_{Fe} are the quantities of Fe ions found in the solutions for uncovered and covered metal surfaces, respectively.

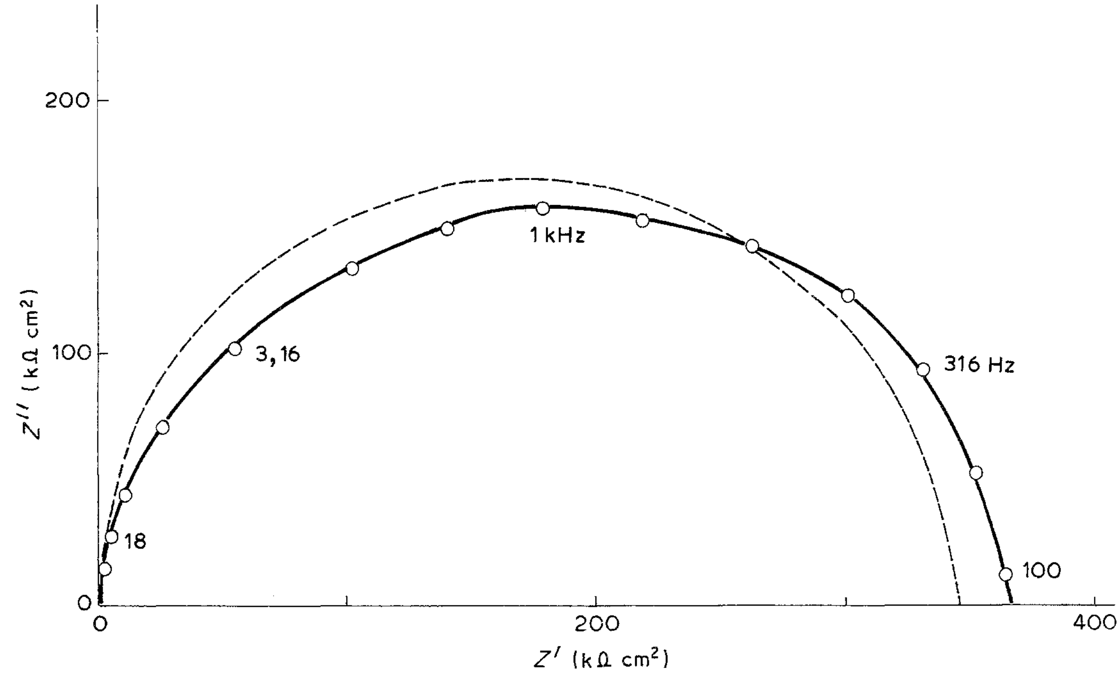

Fig. 12. Nyquist plots for copolymer film obtained at -1.2 V. Theoretical curve is obtained using parameters from Fig. 11.

Figure 13 shows that η_p depends both on the potential of film formation and on the thicknesses of the copolymer films (or time of film formation at a given potential). Unsatisfactory values of corrosion protection efficiency of these films, which can be attributed to the appreciable porosity of the films, were found.

Efforts are in progress to diminish the copolymer film porosity mainly due to the intensive hydrogen evolution reaction.

4. Conclusions

(1) *Ex situ* impedance measurements of cross-linked polymer (PAA) and copolymer (PAA–PAN) films indicate a strong influence of the moisture in the films and/or of the thermal treatments of the films. In the presence of a considerable amount of moisture in the films their impedance characteristics can be determined using an equivalent circuit proposed for *in situ* behaviour of covered metals in corrosion media.

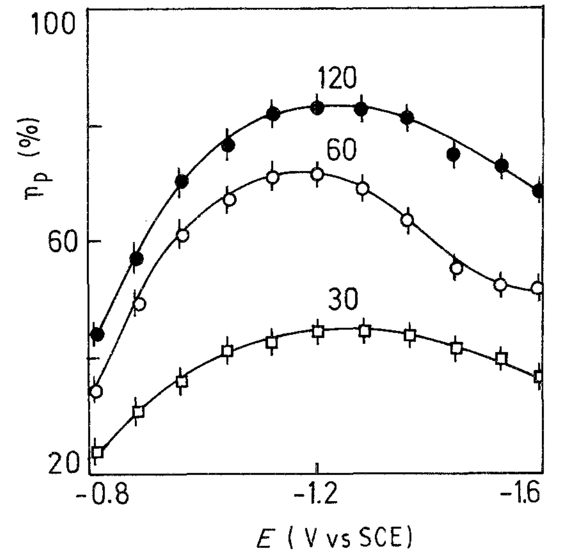

Fig. 13. Corrosion protection efficiency of copolymer films on a steel surface in 3% NaCl solution as a function of potential and time of film formation.

Bode and Nayquist plots clearly show that progressive drying of polymer films strongly changes their impedance behaviour. For a dry polymer film a simple parallel RC circuit can be satisfactorily applied.

The parameters used to construct the theoretical curves of best fit with the experimental data were obtained. It appears that the experimental curves cannot be reproduced using a substantially different set of parameters.

(2) Voltammograms and double-layer capacity measurements on a steel cathode covered with copolymer film indicate the presence of pores in the film, mainly due to the hydrogen evolution reaction taking place simultaneously with the process of copolymer film formation.

(3) The rate of PAA film growth, obtained by EIP of AA in the presence of $ZnCl_2$ on a steel cathode, is about 10^3 nm s^{-1} and that of copolymer (PAA–PAN) film growth only about 1 nm s^{-1}. Such a significant difference can be attributed to the various mechanisms of initiation of the polymerization.

(4) Ellipsometry can be used for the determination of the kinetics of copolymer film formation and double layer capacity measurements for the kinetics of the metal surface covered with copolymer films.

(5) The corrosion protection efficiency of copolymer (PAA–PAN) films tested in 3% NaCl solution strongly depends on the experimental parameters (potential, time, etc) and in the best case reaches about 80%, which is not satisfactory.

Our present investigations at a rotating disc electrode seem promising. Their aim is the avoidance of hydrogen bubble formation on the metal surface.

Acknowledgements

We thank Prof. J. W. Schultze and Dr M. M. Lohrengel for many helpful discussions and equipment support for capacitance measurements.

References

[1] G. L. Collins and N. W. Thomas, *J. Polym. Sci., Polym. Chem. Ed.* **15** (1977) 1819.

[2] Ja. Zitner, K. A. Makarov and O. K. Lebetkina, *Izv. Vyssh. Uchebn. Zaved. Khim. Khim. Tekhnol* **23** (1980) 1532.

[3] M. Cvetkovska, T. Grchev, Lj. Arsov and G. Petrov, *Kem. Ind.* **34** (1985) 235.

[4] T. F. Otero *et al.*, International Workshop, Electrochemistry of Polymer Films, 'Ext. Abst.', Duisburg (1986) p. 3.3.

[5] A. Z. Trifonov and I. D. Schopov, *J. Electroanal. Chem.* **35** (1972) 415.

[6] F. S. Teng, R. Mahalingam, R. V. Subramanian and R. A. Raff, *J. Electrochem. Soc.* **124** (1977) 995.

[7] F. S. Teng and R. Mahalingam, *J. Appl. Polym. Sci.* **23** (1979) 101.

[8] T. Grchev and M. Cvetkovska, 37th ISE Meeting, 'Ext. Abst'. 07-20(I), Vilnius (1986).

[9] M. M. Lohrengel, K. Schubert and J. W. Schultze, *Werkst. Korros.* **32** (1981) 13.

[10] S. P. Papkov, 'Polimernie voloknistie materiali', izd. Himia, Moskva (1986) p. 194.

[11] I. Rubinstein, J. Rishpon and S. Gottesfeld, *J. Electrochem. Soc.* **133** (1986) 729.

[12] W. Fischer and W. Mader, International Workshop, Electrochemistry of Polymer Films, 'Ext. Abst.', Duisburg (1986) p. 3.2.

[13] M. M. Musavi, C. Pagura and G. Mengoli, *Electrochim. Acta.* **30** (1985) 501.

[14] G. W. Walter, *Corros. Sci.* **26** (1986) 681.

[15] F. Mansfeld, S. L. Jeanjaquet and M. W. Kendig, *Corros. Sci.* **26** (1986) 735.

[16] J. C. Padget and P. J. Moreland, *J. Coat. Technol.* **55** (1983) 39.